ELSEVIER

Biophysical Chemistry 129 (2007) 259–268

Biophysical Chemistry

http://www.elsevier.com/locate/biophyschem

Fundamental studies of the cytochrome *c* immobilization by the potential cycling method on nanometer-scale nickel oxide surfaces

Abdolmajid Bayandori Moghaddam [a], Mohammad Reza Ganjali [a,*], Rassoul Dinarvand [b], Ali Akbar Saboury [c], Taherehsadat Razavi [a], Ali Akbar Moosavi-Movahedi [c], Parviz Norouzi [a]

[a] *Center of Excellence in Electrochemistry, Faculty of Chemistry, University of Tehran, P. O. Box: 14155-6455, Tehran, Iran*
[b] *Medical Nanotechnology Research Centre, Medical Sciences/ University of Tehran, Tehran, P.O. Box 14155-6451, Iran*
[c] *Institute of Biochemistry and Biophysics, University of Tehran, Tehran, Iran*

Received 12 April 2007; received in revised form 13 June 2007; accepted 14 June 2007
Available online 22 June 2007

Abstract

This work describes the performance of cytochrome *c*/nickel oxide nanoparticles/glassy carbon electrode, prepared by the electrochemical deposition of the nickel oxide nanoparticles (NiO NPs) on the glassy carbon (GC) electrode surface and the cytochrome *c* immobilization on the nickel oxide nanoparticle surfaces. An extensive sample examination with the help of the SEM and AFM presented the existence of different geometrical shapes of the nickel oxide particles. These geometrical structures could lead to the better immobilization of proteins on their surfaces. The resulting electrode displayed an excellent behavior for the redox of the cytochrome *c*. Also, the resulting heme protein exhibited a direct electrical contact with the electrode because of the structural alignment of the heme protein on the nanometer-scale nickel oxide surfaces. This method could be suitable for applications to nanofabricated devices. In the end, it was concluded that the cytochrome *c* could be tethered to the nanometer-scale nickel oxide surfaces.

Keywords: Cytochrome *c*; Atomic Force Microscopy; Scanning Electron Microscopy; Nanoparticle; Nickel oxide; Nanoelectrochemistry; Bioelectrochemistry

1. Introduction

Bioelectrochemistry is an interdisciplinary field, which combines biotechnology with the electrochemical discipline. This field started to attract the researchers' attention when the existing resemblance between the electrochemical and biological reactions became evident. In fact, it was realized that the oxidation mechanisms on the electrode and in the body share similar principles. On the other hand, the appearance of nanotechnology was opening a new entrance for the performance of this field. Subsequently, it was obvious that the essential coordination of these scientific branches could lead to fruitful findings.

As far as nano-materials are concerned, they offer attractive properties and they have opened a new entrance for new electrodes in the field of electrochemical applications [1]. The nano-scale effects in the catalytic properties of gold particles are well-known chemically inert. Gold turns catalytically active when the particle size is below 3–4 nm [2,3]. Electrodes with nanometer dimensions provide exciting new tools for electrochemical studies. The small dimensions lead to a high current density on the electrode surface, allowing the study of the fast heterogeneous electron transfer kinetics, the molecular interactions and the mass transport in the nanometer regime [4]. The existence of nano-size effects offers a new possibility to control reactivity by controlling the particle size. Exploiting the small dimensions of nanoelectrodes may allow innovative biological applications by means of entering local cellular environments and ultimately measuring the activity of a single redox-enzyme coupled to a nanoelectrode.

Regarding the fundamental investigations of the biological redox reaction mechanism and the development of biosensors and bioelectronic devices, the achievement of an interface between the prosthetic groups of immobilized proteins/enzymes

* Corresponding author. Tel.: +98 21 61112788; fax: +98 21 66405141.
E-mail address: Ganjali@khayam.ut.ac.ir (M.R. Ganjali).

0301-4622/$ - see front matter © 2007 Elsevier B.V. All rights reserved.
doi:10.1016/j.bpc.2007.06.006

of redox proteins and an electrode surface is presently a research frontier [5–14]. The redox reaction kinetics of proteins on an electrode are known to be strongly dependent upon a combination of interfacial electrostatic and chemical interactions, which are derived from the protein structure and the nature of the electrode surface. In this way, the biosensors and the bioelectronic devices can be simplified without the usage of chemical mediators and a model can be designed for the electron transfer study between proteins or enzymes in real living systems.

Many enzymes exchange electrons with small redox proteins, like cytochrome *c*. Cytochrome *c* is a water-soluble heme protein that exists in the cytosol between the inner and outer membranes of mitochondria. Its Fe(III)/Fe(II) redox center is located at a heme unit which is approximately spherical in shape with 34 Å, while its crystallographic dimension is $3.0 \cdot 4.0 \cdot 3.0$ nm [12]. Additionally, it plays an important role in the biological respiratory chain. In fact, its function is to receive electrons from the cytochrome *c* reductase and deliver them to the cytochrome c oxidase. Initially, redox proteins (e.g. cytochrome *c*) were believed to be incapable of exhibiting a voltammetric response, because of the extremely slow electron-transfer kinetics at the electrode/solution interface. However, in 1977, Yeh and Kuwana reported a direct and rapid electron transfer between cytochrome *c* and a tin-doped indium oxide electrode surface [15]. In the same year, Hill and Eddowes demonstrated that the voltammetry of cytochrome *c* was well defined at a gold electrode modified with 4,4′-bipyridil [16].

Since that time, electrochemical devices have introduced new possibilities for the study of the redox process of cytochrome *c* and related heme proteins [17–19]. Many reports have described the electrochemistry of cytochrome *c* in terms of modifier electrode and modifier-protein interactions [20–27]. Many promoters, such as some small organic compounds [28–31], amino acids together with some derived molecules [26,27], small peptides [32] and conductive polymers [33], have been found to promote the direct electrochemistry of cytochrome *c* on the electrode surface. Recently, the matrices used for the cytochrome *c* immobilization are a series of inorganic porous [34–36] and nano-materials [37–42].

Various ionic liquids have been combined with carbon nanotubes to form a conductive gel, which can be employed to investigate the cytochrome *c* electrochemical behavior [43,44]. The mitochondrial cytochrome *c* has shown to be spontaneously adsorbed on carbon nanotubes [45–48]. The interaction most likely occurs via the protein side that is rich in Lys residues, since the primary amines strongly bind to carboxylate functionalities [49–52]. Furthermore, amines are also known to strongly interact with the carbon nanotube sidewall [53–55]. Because the heme group slightly protrudes into the solution on that side, this orientation is very favorable for fast electron exchange. Unfortunately, the same Lys-rich side of cytochrome *c* is also the docking side for the enzymes [56–61].

A literature survey revealed that several studies [62–93] have been devoted to the investigation of the nickel electrode electrochemistry for a number of applications: the nickel-cadmium batteries [62–84], as a model for studying the oxygen-evolution reaction [62–65], the oxidation of the organic compounds at the passivated nickel anodes [66] as well as the electroanalytical approach based on the interaction of sulphide with an electrochemically generated nickel oxide layer [67–85]. Moreover, the production of the different phases of the nickel sulphide nanocrystals from the reaction of the nickel metal nanoparticles supported on graphitized carbon with hydrogen sulphide [86], an anodic stripping voltammetric method for the sub-speciation of Ni_3S_2, NiS and NiS_2 in the mixtures of carbon paste electrodes in an acetate buffer [87] and the electrochemically deposited nickel microparticles onto a carbon substrate for sulphide detection [88]. Finally, the modification of glassy carbon electrode by the nickel oxide nanoparticles for the immobilization of hemoglobin, catalase and glucose oxidase [89–91] and the use of Ni/NiO for the preparation of silicon nanotube array/gold electrode for the direct electrochemistry of cytochrome *c* are the studies that complete the applications of this category [92].

In total, this paper introduces an electrochemical investigation on the redox reaction of the immobilized cytochrome *c* as cytochrome *c*/nickel oxide nanoparticles/glassy carbon electrode (Cyt *c*/NiO NPs/GC electrode).

2. Experimental details

2.1. Chemicals and reagents

Cytochrome *c* [EEC NO 232-700-9] was purchased from Sigma. The phosphate buffer solution (PBS) consisted of a potassium phosphate solution (KH_2PO_4 and K_2HPO_4 from

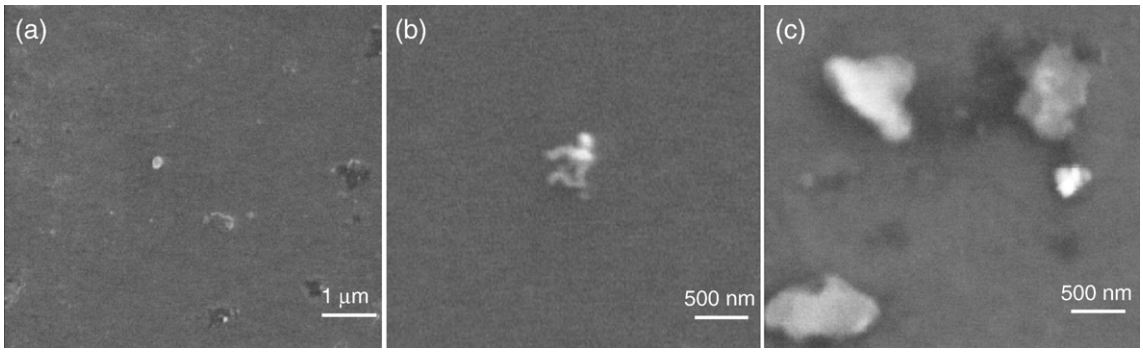

Fig. 1. (a–c) The SEM images of the electrodeposited ($E = -0.80$ V, $t = 5$ min deposition time) nickel oxide nanoparticles on the GC electrode surface.

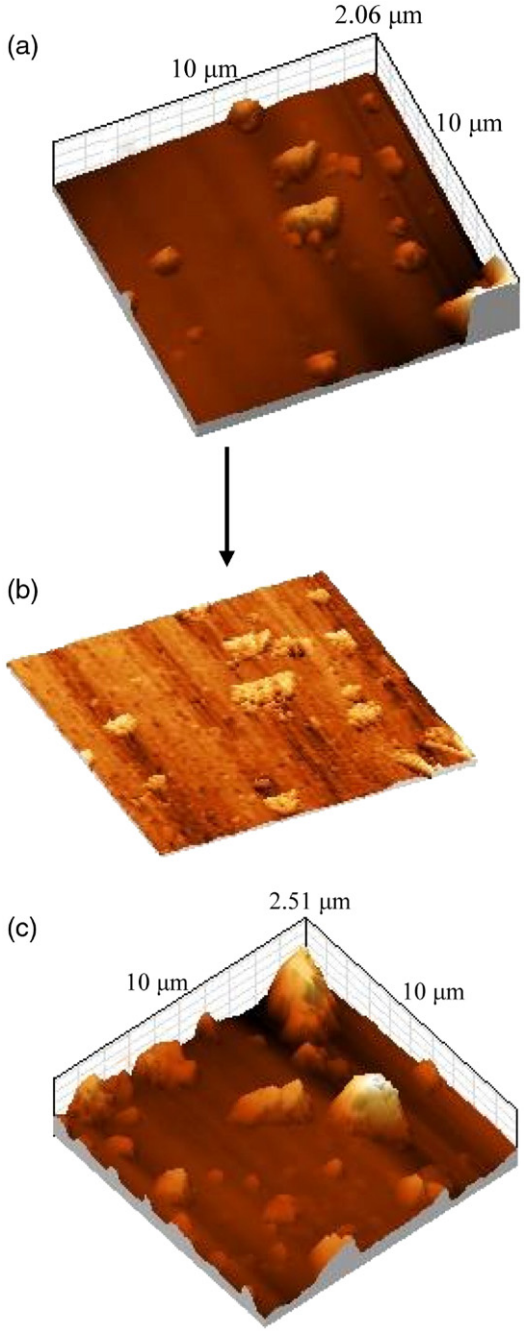

Fig. 2. (a–c) The AFM images of the electrodeposited nickel oxide nanoparticles on the GC electrode surface.

Merck; 0.05 M total phosphate) at pH 7.0. An acetate buffer solution (CH_3COONa and CH_3COOH from Merck; 0.05 M) was freshly prepared. $Ni(NO_3)_2{\cdot}6H_2O$ and the other reagents were reagent grade materials from Merck. Deionized water was used to prepare all solutions and to rinse the electrodes.

2.2. Electrochemistry

All electrochemical experiments were performed by the Autolab potentiostat PGSTAT 30 (Eco Chemie B.V., Netherlands), equipped with the GPES 4.9 software. The Q value for each point of the continuous CVs was obtained from the formula $Q = \int_0^t idt$, $Q_1 = i_1 \Delta t$, $Q_2 = (i_1 + i_2)\ \Delta t$, $Q_n = \sum_{k=1}^{k=n} i_k \Delta t$. Then we created the plots of Q *vs.* E and Q *vs.* time.

A three-electrode cell was also used, employing a glassy carbon (GC) electrode or modified-GC electrodes, acting as the working electrodes. A platinum wire was applied as the counter electrode and Ag|AgCl|KCl (sat.) was applied as the reference electrode. All potentials were reported with respect to this reference. All experiments were performed at 25 ± 1 °C.

Prior to the cytochrome *c* immobilization, the glassy carbon electrode (1 mm in diameter) surface along with the alumina slurry surfaces of 1.0, 0.3 and 0.05 μm were polished, the former to a mirror-like one with fine emery papers and the latter with a polishing cloth, followed by a thorough deionized water rinsing. The electrode was then successively sonicated in ethanol and doubly distilled water to remove the adsorbed particles. Then, cyclic scans were carried out in PBS (0.05 M, pH 7.0) in the potential range from −0.50 to 1.0 V, until the repetitive cyclic voltammograms (CVs) were obtained. The solution, in which the nickel deposition was conducted, typically consisted of 15 mL acetate buffer (pH 4.0). The nickel was initially electrodeposited (−0.80 V, 5 min. deposition time) on a GC electrode from a 1 mM nickel nitrate pH 4.0 acetate buffer solution. The use of more than 5 min deposition time was due to the growth of the NiO NPs to larger sizes (NiO microparticles), which are not suitable for the modification of the GC electrode. Afterwards, the Ni-GC electrode was placed into a fresh PBS (pH 7.0) and electrochemically passivated with the potential cycling method (protocol for the NiO NPs/GC electrode) [84,85,88]. In another protocol, the Ni–GC electrode was placed into a fresh PBS including 5 mg mL^{-1} cytochrome *c*. Then, the Ni–GC electrode was electrochemically passivated and the cytochrome *c* was immobilized with the aid of the potential cycling method (protocol for the Cyt *c*/NiO NPs/GC electrode) [84,85,88–90]. The potentials were repetitively cycled (30 scans) from 1.0 V to −0.50 V at a scan rate of 100 mV s^{-1}. Finally, the modified electrodes were washed in deionized water and placed in PBS (PH 7.0) at a refrigerator (3–5 °C), before being employed in the electrochemical measurements as the working electrode.

3. Results and discussions

3.1. Scanning Electron Microscopy (SEM) and Atomic Force Microscopy (AFM)

As it is well known, the properties of a broad range of materials and the performance of a large variety of devices depend strongly on their surface characteristics. For instance, the surface of a biomaterial/biomedical device meets the physiological environment, immediately after it is placed in the body or bloodstream and the initial contact regulates its subsequent performance [94].

Fig. 1 shows the scanning electron microscopic images of the nanometer-scale nickel oxide particles, generated on the GC electrode surface in different distances from each other in various sizes. On the grounds that the surface-to-volume ratio increases with the size decrease and because of the fact that the

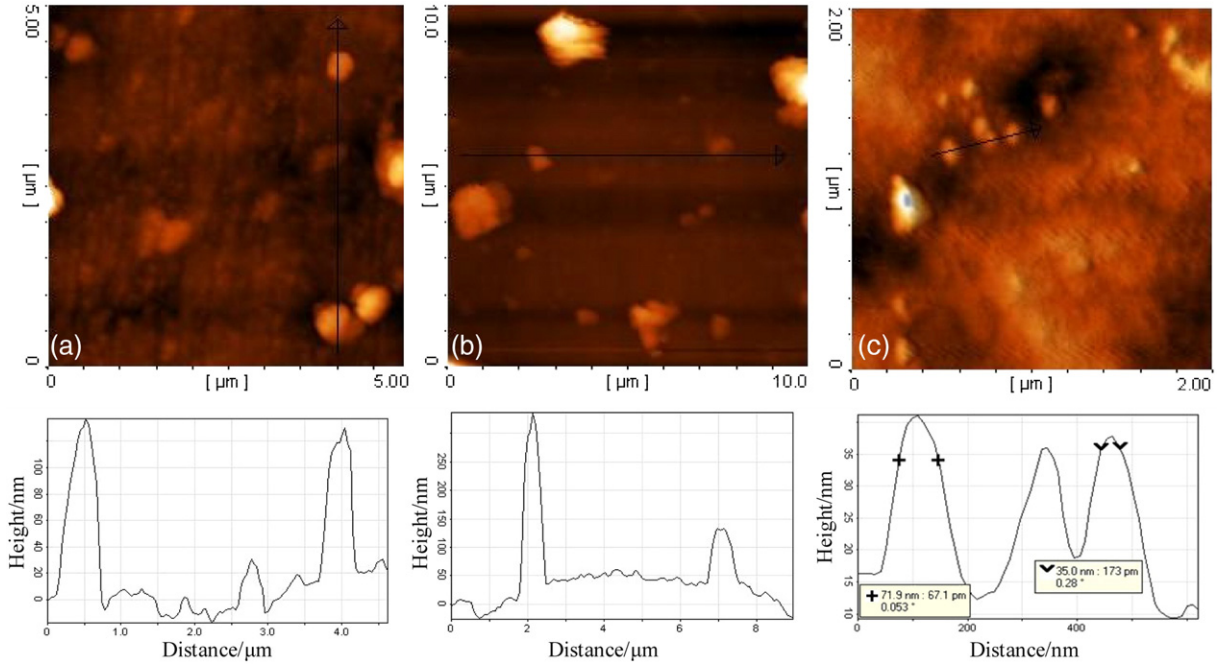

Fig. 3. (a–c) The AFM images and the obtained image profiles of the electrodeposited nickel oxide nanoparticles on the GC electrode surface.

size of proteins is comparable with the nanometer-scale building blocks, the smaller nanoparticles can play a very important role during the immobilization process.

Actually, the SEM technique presents limitations for such investigations at higher resolutions, to overcome this problem and because the SEM results suggest only nanoparticle structure existence (and not a detailed structure of these nanoparticles), it was useful to inspect this issue by means of another nanotechnological technique. For the structure investigation of these nanoparticles and, mainly, the smaller ones (which were not investigated in the SEM studies), the atomic force microscopy (AFM) provided an excellent opportunity. Figs. 2 and 3 present the AFM images of the nanometer-scale nickel oxide particles. Correspondingly, an extensive sample examinations with the help of the SEM and AFM techniques have exhibited the existence of different geometrical shapes of nickel oxide particles. Fig. 3a–c demonstrate both the AFM images and the image profiles of these particles. These profiles displayed that the nanoparticle diameters have decreased on the top, contrary to the bottom of the nanoparticles (similar to a needle). These geometrical structures can show a significant effect for the better immobilization of proteins on their surfaces. In line with our investigations after the SEM and AFM utilization, the diameter of the nanometer-scale nickel oxide particles was about 80 nm to 900 nm (however, some of them exhibited a diameter of about 1.0 to 1.2 µm).

3.2. Passivation of the nickel oxide nanoparticles and the cytochrome c immobilization

The dissolution and passivation of the deposited nickel on the GC electrode in PBS (PH 7.0) were first investigated with the help of the potential cycling method, 10 cycles, being depicted in Fig. 4. The observed oxidative wave at the first CV corresponded to the active anodic dissolution of nickel and the anodic current was probably due to the existence of a protective film formed by the oxide species [67,70–75,85], known as an active-passive transition state. The second CV revealed a negligible anodic current occurring. This indicated that the complete nickel passivation could be achieved within 2 cycles and, consequently, stable voltammetric responses were observed. There were no reduction waves, indicating that the passive nickel oxide nanoparticles were retained. Afterwards, the next CVs (third to tenth) were placed under the first two CVs, illustrating that no further nickel dissolution had taken place. Therefore, the formed passive nickel oxide nanoparticles were stable within the studied potential window.

In the electrochemical investigations of the cytochrome *c* immobilization on the nickel oxide nanometer-scale surfaces, a potential cycling (30 cycles) was applied to the electrodeposited

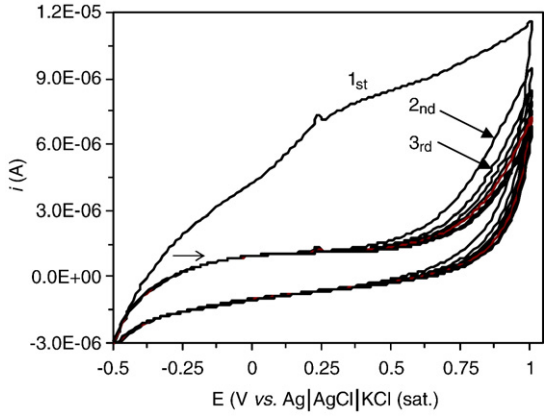

Fig. 4. The first 10 CVs of the deposited nickel on the GC electrode after being placed in PBS (pH=7.0), scan rate; 100 mV s^{-1}.

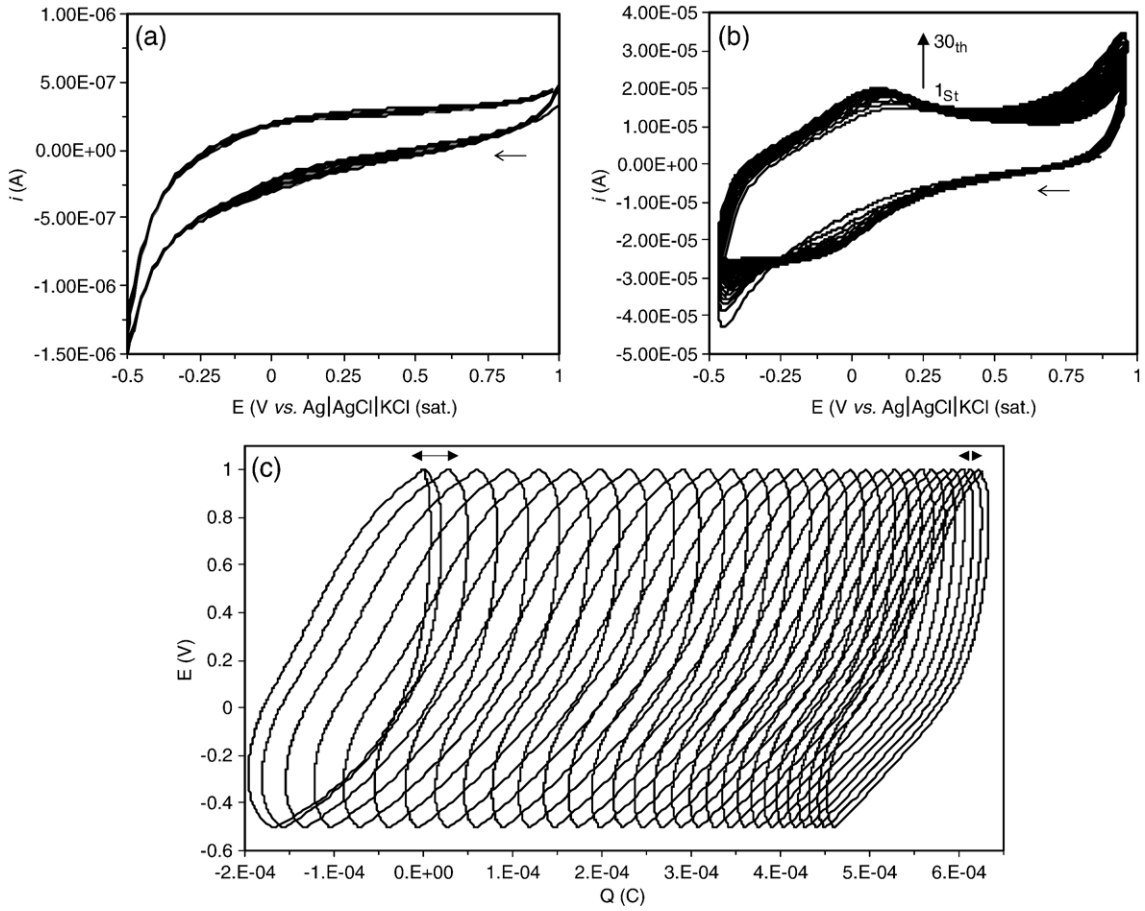

Fig. 5. NiO passivation (a), NiO passivation and cytochrome *c* immobilization (b) by the potential cycling method (30 cycles) in PBS (pH = 7.0), scan rate; 100 mV s^{-1}, and (c) the potentials (E) *vs.* the charge passed through the electrochemical cell for the simultaneous passivation of the deposited metallic nickel and the cytochrome *c* immobilization in PBS. The data were obtained for 30 cycles (CVs presented in Fig. 5b).

(−0.80 V, 5 min. deposition time) metallic nickel in the absence and presence of cytochrome *c*, between 1.0 to −0.50 V in PBS (pH 7.0) at the scan rate of 100 mV s^{-1}. Fig. 5a demonstrates the acquired CVs in PBS (pH 7.0) for the deposited metallic nickel on the GC electrode, where no electrochemical activities occured. Fig. 5b shows the generated CVs under the same conditions in the fresh PBS, including 5 mg mL^{-1} cytochrome *c*. It is clear from Fig. 5b that the anodic and cathodic peak current increased with the increase of the cycles, being related to the electrochemical oxidation and reduction of the immobilized cytochrome *c* on the nickel oxide nanometer-scale surfaces. The immobilized cytochrome *c* has increased with the increasing of the cycles and the increase in the anodic and cathodic peak currents, related to this phenomenon. The result from this procedure was the simultaneous formation of the nanometer-scale nickel oxide surfaces and the cytochrome *c* immobilization on these surfaces. Afterwards, the cytochrome *c* covered the nanometer-scale nickel surfaces and the stable CVs were observed. With the cycle number increase, the increase in the anodic and cathodic peak currents diminished. This phenomenon has become more evident from the plot of *E vs. Q* in Fig. 5c. In this figure, the distances among the rings have decreased with the consumed charges (*Q*) increase, in accordance with the increase of the immobilized cytochrome *c* and the decrease of the bare nanometer-scale nickel oxide surfaces. Furthermore, the charge passed through the electrochemical cell (*Q*, consumed charge) has been compared with the time for the passivation of the deposited metallic nickel (Fig. 6a, data obtained from the CVs of Fig. 5a), as well as the passivation of the deposited metallic nickel and the cytochrome *c* immobilization on the

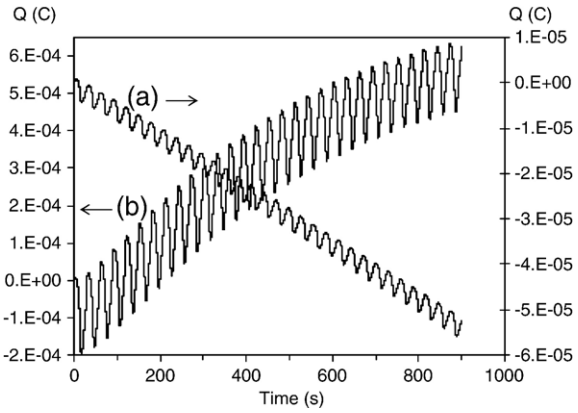

Fig. 6. The charge passed through the electrochemical cell *vs.* time for (a) the passivation of the deposited metallic nickel in PBS (CVs presented in Fig. 5a), (b) the passivation of the deposited metallic nickel and the cytochrome *c* immobilization in PBS (CVs presented in Fig. 5b).

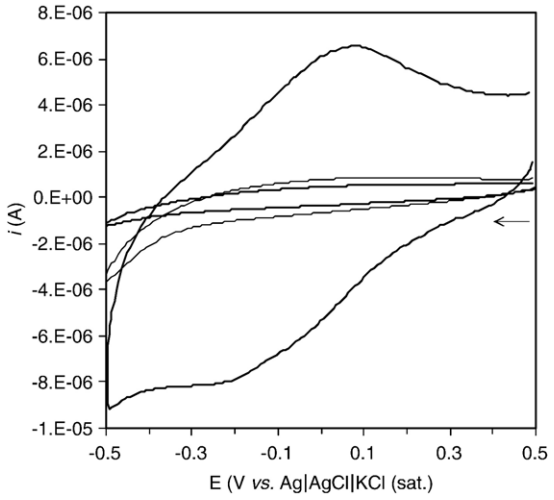

Fig. 7. CVs in PBS (pH 7.0, 0.05 M) from inner to outer; NiO NPs/GC electrode, the GC electrode and the Cyt *c*/NiO NPs/GC electrode, scan rate; 100 mV s^{-1}.

nickel oxide nanometer-scale surfaces simultaneously (Fig. 6b, data obtained from the CVs of Fig. 5b). In accordance with Fig. 6, the consumed charge (Q) presented slight changes during the cycles, being attributed to the passivation of the deposited metallic nickel on the GC electrode. Nonetheless, it illustrated considerable changes during the simultaneous passivation and immobilization. The amount of Q for the simultaneous passivation and immobilization procedure was more than the respective one for only the passivation procedure in each cycle. However, the amount of Q was rinsed to steady state after about 30 cycles, because the nanometer-scale nickel oxide surfaces were covered by the cytochrome *c*.

3.3. Direct voltammetric behavior of the Cyt c/NiO NPs/GC electrode

The integrity of the immobilized cytochrome *c* construction and its ability to exchange electrons with the nanometer-scale nickel oxide particle surfaces have been assessed by voltammetry. A macroscopic electrode was required to attain a large enough cytochrome *c* sample to yield detectable direct oxidation and reduction currents. The comparative CVs for the GC, NiO NPs/GC (the GC electrode was modified with the nanometer-scale nickel oxide particles) and Cyt *c*/NiO NPs/GC electrodes in 0.05 M PBS (pH 7.0) was obtained. These voltammograms are demonstrated in Fig. 7. From this Figure, it has been noticed that there were no voltammetric responses at both bare GC and GC–NiO electrodes, indicating that the GC and NiO NPs/GC electrodes were electroinactive in the studied potential window. However, Fig. 7 depicts a well-defined pair of oxidation-reduction (redox) peaks, observed at the Cyt *c*/NiO

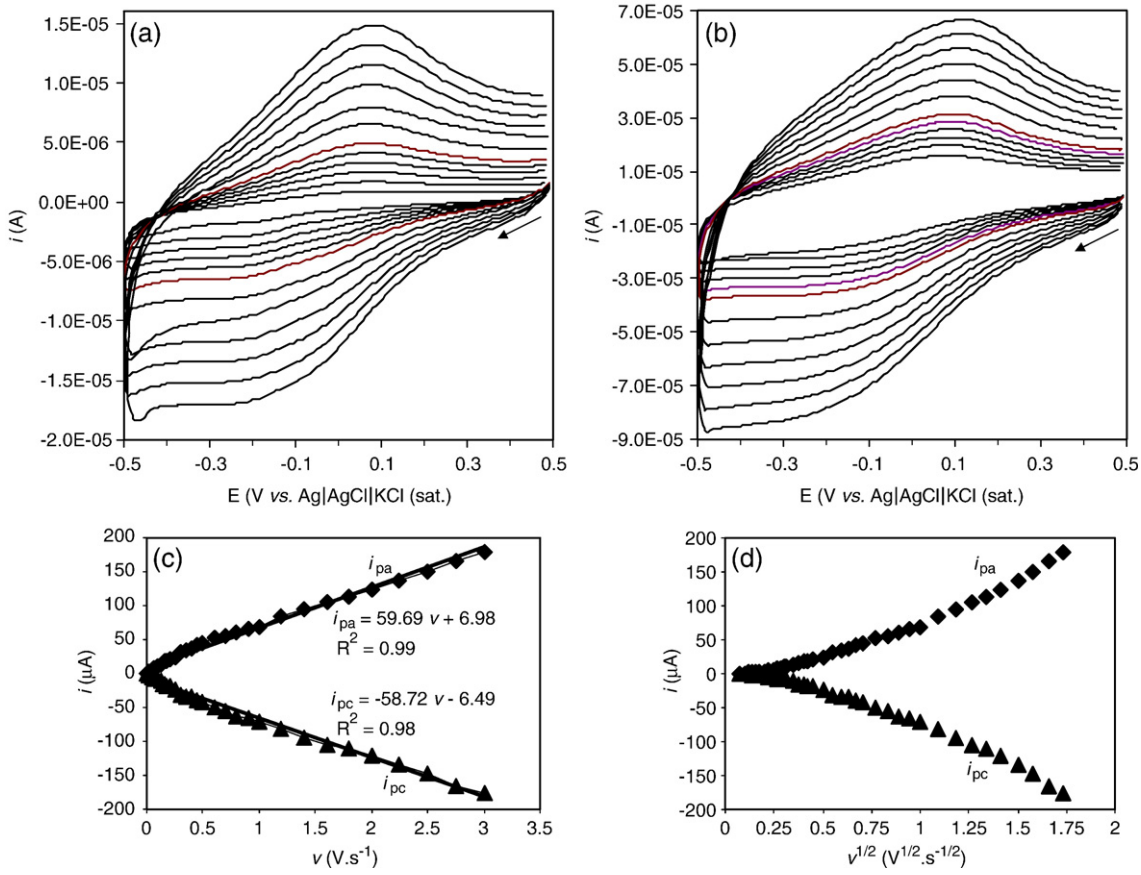

Fig. 8. CVs of Cyt *c*/NiO NPs/GC electrode in PBS (pH 7.0, 0.05 M) at various scan rates, from inner to outer; (a) 5, 10, 15, 20, 25, 30, 40, 50, 60, 70, 80, 90, (b) 100, 120, 140, 160, 180, 200, 250, 300, 350, 400, 450, and 500 mV s^{-1}.

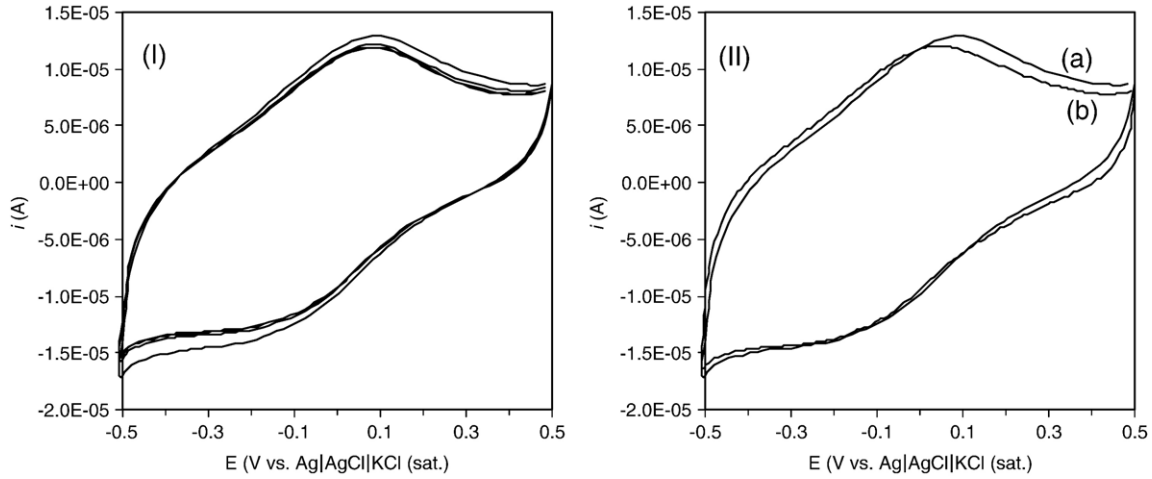

Fig. 9. (I) Continuous CVs of Cyt *c*/NiO NPs/GC electrode, from outer to inner the first, 50th, 100th, and 250th CV for the fresh electrode. (II) Obtained CVs for fresh (*a*), and reserved electrode for the 2 weeks, scan rate: 100 mV s^{-1}, other conditions as in Fig. 8.

NPs/GC electrode at the scan rate value of 100 mV s^{-1}. The Cyt *c*/NiO NPs/GC electrode presented the reductive peak potential at −0.202 V, the corresponding oxidative peak potential at 0.058 V, revealing the adsorbed cytochrome *c* on the nanometer-scale nickel oxide particle surfaces. The difference of anodic and cathodic peak potential values was $\Delta E = 0.261$ V. These redox peaks were attributed to the redox reaction of the cytochrome *c* electroactive center. The formal potential ($E^{\circ\prime}$) for the cytochrome *c* redox reaction on the Cyt *c*/NiO NPs/GC electrode was −0.072 V with respect to the reference electrode. "The formal potential values for horse cytochrome *c* and yeast cytochrome *c* on the indium/tin oxide (ITO) were −0.028 V and −0.048 V, respectively [95]. This value was −0.16 V for the gold nanoparticles-chitosan-carbon nanotubes [96]". In agreement with the collected voltammograms in Fig. 7, it was concluded that the nanometer-scale nickel oxide particles could play a key role in the observation of cytochrome *c* CV response. These nanoparticles have displayed a great effect on the electron exchange assistance between cytochrome *c* and the GC electrode.

To further investigate the cytochrome *c* characteristics at the Cyt *c*/NiO NPs/GC electrode, the effect of scan rates on the cytochrome *c* voltammetric behavior have been studied in detail and the kinetic parameters have been acquired. Fig. 8 (a and b) depicts the CVs for the immobilized cytochrome *c* at various scan rates. The scan rate (v) and the square root scan rate ($v^{1/2}$) dependence of the heights and potentials of the peaks are plotted in Fig. 8 (c and d). It can be seen that the redox peak currents have increased linearly with the scan rate, the correlation coefficient was 0.98 ($i_{pc} = -58.72\,v - 6.49$) and 0.99 ($i_{pa} = 59.69\,v + 6.98$), respectively. This phenomenon implied that the redox process is an adsorption-controlled and the immobilized cytochrome *c* has been stable.

It was found that with the scan rate increase, the oxidation peak shifted to more positive potentials, while the reduction peak shifted to potentials that were more negative. The anodic and cathodic peak potentials are linearly dependent on the logarithm of scan rates (v) when $v > 1.0$ V.s^{-1}, which was in agreement with the Laviron theory, with slopes of $-2.3RT/\alpha nF$ and $2.3RT/(1-\alpha)nF$ for the cathodic and the anodic peak, respectively [97]. As a result, the charge-transfer coefficient (α) can be estimated as 0.64 from the slope of the straight lines based on the equation:

$$\log(v_a/v_c) = \log[\alpha/(1-\alpha)] \text{ or } (v_a/v_c) = [\alpha/(1-\alpha)] \quad (1)$$

The heterogeneous electron transfer rate constant (k_s) can be estimated according to the following equation [97,98]:

$$\log k_s = \alpha \log(1-\alpha) + (1-\alpha)\log \alpha - \log\frac{RT}{nFv} - \frac{\alpha(1-\alpha)nF\Delta E_p}{2.303RT} \quad (2)$$

Here n is the number of electrons transferred in the rate determining reaction, R, T and F symbols have their conventional meanings and ΔE_p is the peak potential separation. The ΔE_p values were 0.269, 0.276 and 0.282 V at 0.15, 0.20, and 0.25 V s^{-1} respectively, giving an average heterogeneous transfer rate constant (k_s) value of 0.29 s^{-1}. It was less than that of cytochrome *c* adsorbed on colloidal Au (1.21 ± 0.08 s^{-1}) [41], the NaY zeolite (0.78 ± 0.04 s^{-1}) [35] and very near to that of ordered mesoporous niobium oxide film (0.28 s^{-1}) [34].

3.4. Stability of the immobilized cytochrome c on the nanometer-scale nickel oxide surfaces

Stability is a very significant characteristic in biodiagnostics. The stability of the immobilized cytochrome *c* on the nanometer-scale nickel oxide surfaces on the Cyt *c*/NiO NPs/GC electrode has been evaluated by voltammetry. The peak height and the peak potential of the Cyt *c*/NiO NPs/GC electrode remained approximately unchanged during the long duration of the continuous cyclic voltammograms between 0.50 to −0.50 V. The surface area under the 50th voltammogram was almost 4.5% smaller than the surface area under the first voltammogram. This difference reduced to 0.5% for the same comparison for the 50th and 100th voltammograms. There were no differences between the 100th and 250th voltammograms at the scan rate value of 100 mV s^{-1}, because the surface area under the CV indicated the consumed charge (Q), related to the

amount of the immobilized cytochrome *c*. Therefore, the amount of the immobilized cytochrome *c* on the nanometer-scale nickel oxide surfaces, after the 50th cycle, was about 96.5% of the initial value at the first cycle, equivalent to 96% for the 100th to 250th cycles.

In another procedure, the Cyt *c*/NiO NPs/GC electrode was placed in 0.05 M PBS (pH 7.0, 3–5 °C) for 2 weeks. In the end of this period, the voltammograms at 100 mV s^{-1} in fresh 0.05 M PBS (pH 7.0) were recorded. Fig. 9 (II) demonstrates these voltammograms. Specifically, Fig. 9 (II)b presented that there were no changes in the reduction potential and the reduction peak height. Regarding the oxidation peak, the oxidation peak height diminished. Additionally, it was noticed that the oxidation process occured at a lower potential value after the 2 week period. In other words, the oxidation process took place with greater convenience. Owing to the decrease in the ΔE_p ($E_{pc} - E_{pa}$), the reversibility was better than before. Subsequently, the electrical contact was better after 2 weeks. This observation could be attributed to some cytochrome *c* rearrangements on the nanometer-scale nickel oxide surfaces, based on the better electrical contact of the cytochrome *c* prosthetic groups with the nanometer-scale nickel oxide surfaces.

4. Conclusions

It was presented that the nanometer-scale nickel oxide surfaces were useful for the cytochrome *c* stable entrapment. After the demonstration of an excellent behavior towards the cytochrome *c* redox by the recommended electrode, the direct electron transfer of cytochrome *c* on Cyt *c*/NiO NPs/GC was achieved.

Undoubtedly, nanotechnology in combination with bioelectrochemistry can extremely influence the development rate of these scientific fields. However, a number of challenges remain to be faced, which are related to the processing of the electrode modifications in a more controlled method. We are still at an early stage of understanding the fundamental theories of the bioelectrochemical systems. The charge transport mechanism in nanostructured biointerfaces remains a fascinating subject and needs to be additionally explored.

Nevertheless, the recent advances have been important for the comprehension of the nanostructured biointerfaces. As a result, it will be possible to more effectively reach the frontiers of the modern material science, including bioelectronics, biocatalysis and biosensing.

References

[1] A. Bayandori Moghaddam, M.R. Ganjali, R. Dinarvand, P. Norouzi, A.A. Saboury, A.A. Moosavi-Movahedi, Electrochemical behavior of caffeic acid at single-walled carbon nanotube:graphite-based electrode, Biophys. Chemist. 128 (2007) 30–37.
[2] M. Haruta, Novel catalysis of gold deposited on metal oxides, Catal. Today 36 (1997) 153–166.
[3] M. Valden, X. Lai, D.W. Goodman, Onset of catalytic activity of gold clusters on titania with the appearance of nonmetallic properties, Science 281 (1998) 1647–1650.
[4] I. Heller, J. Kong, H.A. Heering, K.A. Williams, S.G. Lemay, C. Dekker, Individual single-walled carbon nanotubes as nanoelectrodes for electrochemistry, Nano Lett. 5 (2005) 137–142.
[5] W. Gopel, P. Heiduschka, Interface analysis in biosensor design, Biosens. Bioelectron. 10 (1995) 853–883.
[6] A.P.F. Turner, Biosensors-sense and sensitivity, Science 290 (2000) 1315–1317.
[7] I. Willner, E. Katz, Integration of layered redox proteins and conductive supports for bioelectronic applications, Angew. Chem., Int. Ed. Engl. 39 (2000) 1180–1218.
[8] J.J. Wei, H.Y. Liu, A.R. Dick, H. Yamamoto, Y.F. He, D.H. Waldeck, Direct wiring of cytochrome c's heme unit to an electrode: electrochemical studies, J. Am. Chem. Soc. 124 (2002) 9591–9599.
[9] Y. Xiao, F. Patolsky, E. Katz, J.F. Hainfeld, I. Willner, "Plugging into Enzymes": nanowiring of redox enzsymes by a gold nanoparticle, Science 299 (2003) 1877–1881.
[10] M.K. Bissenhirtz, F.W. Scheller, W.F.M. Stocklein, D.G. Kurth, H. Mhwald, F. Lisdat, Electroactive cytochrome c multilayers within a polyelectrolyte assembly, Angew. Chem., Int. Ed. Engl. 43 (2004) 4357–4360.
[11] D.A. Moffet, J. Foley, M.H. Hecht, Midpoint reduction potentials and heme binding stoichiometries of de novo proteind from designedcombinatorial libraries, Biophys. Chemist. 105 (2003) 231–239.
[12] Y.-H. Bi, Z.-L. Huang, Y.-D. Zhao, Z.-L. Huang, Y.-D. Zhao, Interactions of cytochrome c with DNA at glassy carbon surface, Biophys. Chemist. 116 (2005) 193–198.
[13] J.-M. Xu, W. Li, Q.-F. Yin, Y.-L. Zhu, Direct electrochemistry of cytochrome c on natural nano-attapulgite clay modified electrode and its electrocatalytic reduction for H_2O_2, Electrochim. Acta 52 (2007) 3601–3606.
[14] X. Jiang, L. Zhang, S. Dong, Assemble of poly(aniline-co-*o*-aminobenzenesulfonic acid) three-dimentional tubal net-works onto ITO electrode and its application for the direct electrochemistry and electrocatalytic behavior of cytochrome c, Electrochem. Commun. 8 (2006) 1137–1141.
[15] P. Yeh, T. Kuwana, Reversible electrode reaction of cytochrome *c*, Chem. Lett. 10 (1977) 1145–1148.
[16] M.J. Eddowes, H.A.O. Hill, Novel method for the investigation of the electrochemistry of metalloproteins: cytochrome *c*, J. Chem. Soc. Chem. Commun. 21 (1977) 771b–772b.
[17] F.A. Armstrong, G.S. Wilson, Recent developments in faradaic bioelectrochemistry, Electrochim. Acta 45 (2000) 2623–2645.
[18] L. Gorton, A. Lindgren, T. Larsson, F.D. Munteanu, T. Ruzgas, I. Gazargan, Direct electron transfer between heme-containing enzymes and electrodes as basis for third generation biosensors, Anal. Chim. Acta 400 (1999) 91–108.
[19] M. Fedurco, Redox reactions of heme-containing metalloproteins: dynamic effects of self-assembled monolayers on thermodynamics and kinetics of cytochrome c electron-transfer reactions, Coord. Chem. Rev. 209 (2000) 263–331.
[20] C.X. Cai, The direct electrochemistry of cytochrome c at a gold microband electrode modified with 4,6-dimethyl-2-mercaptopyrimidine, J. Electroanal. Chem. 393 (1995) 119–122.
[21] S. Arnold, Z.Q. Feng, T. Kakiuchi, W. Knoll, K. Niki, Investigation of the electrode reaction of cytochrome c through mixed self-assembled monolayers of alkanethiols on gold(111) surfaces, J. Electroanal. Chem. 438 (1997) 91–97.
[22] H.A.O. Hill, N.I. Hunt, A.M. Bond, The transient nature of the diffusion controlled component of the electrochemistry of cytochrome c at 'bare" gold electrodes: an explanation based on a self-blocking mechanism, J. Electroanal. Chem. 436 (1997) 17–25.
[23] H. Ohno, K.I. Kato, Electron transfer reaction of cytochrome c at poly(ethylene oxide)-thiolate-modified gold electrode, Chem. Lett. 27 (1998) 407–502.
[24] A.E. Kasmi, J.M. Wallace, E.F. Bowden, S.M. Binet, R.J. Linderman, Controlling interfacial electron-transfer kinetics of cytochrome c with mixed self-assembled monolayers, J. Am. Chem. Soc. 120 (1998) 225–226.
[25] T. Ruzgas, L. Wong, A.K. Gaigalas, V.L. Vilker, Electron transfer between surface-confined cytochrome c and an n-acetylcysteine-modified gold electrode, Langmuir 14 (1998) 7298–7305.
[26] H. Park, J.S. Park, Y.B. Shim, Electrochemical and in situ uv-visible spectroscopic behavior of cytochrome c at a cardiolipin-modified electrode, J. Electroanal. Chem. 514 (2001) 67–74.
[27] K.J. Mckenzie, F. Marken, M. Opallo, TiO_2 phytate films as hosts and conduits for cytochrome c electrochemistry, Bioelectrochemistry 66 (2005) 41–47.

[28] P.M. Allen, H.A.O. Hill, N.J. Walton, Surface modifiers for the promotion of direct electrochemistry of cytochrome c, J. Electroanal. Chem. 178 (1984) 69–86.
[29] S. Song, R.A. Clark, E.F. Bowden, M.J. Tarlov, Characterization of cytochrome c/alkanethiolate structures prepared by self-assembly on gold, J. Phys. Chem. 97 (1993) 6564–6572.
[30] K.D. Gleria, H.A.O. Hill, V.J. Lowe, D.J. Page, Direct electrochemistry of horse-heart cytochrome c at amino acid-modified gold electrodes, J. Electroanal. Chem. 213 (1986) 333–338.
[31] J.M. Cooper, K.R. Greenough, C.J. McNeil, Direct electron transfer reactions between immobilized cytochrome c and modified gold electrodes, J. Electroanal. Chem. 347 (1993) 267–275.
[32] P.D. Barker, K.D. Gleria, H.A.O. Hill, V.J. Lowe, Electron transfer reactions of metalloproteins at peptide-modified gold electrodes, Eur. J. Biochem. 190 (1990) 171–175.
[33] P.N. Bartlett, J. Farington, The electrochemistry of cytochrome c at a conducting polymer electrode, J. Electroanal. Chem. 261 (1989) 471–475.
[34] X. Xu, B. Tian, J. Kong, S. Zhang, B. Liu, D. Zhao, Ordered mesoporous niobium oxide film: A novel matrix for assembling functional proteins for bioelectrochemical applications, Adv. Mater. 15 (2003) 1932–1936.
[35] Z. Dai, S. Liu, H. Ju, Direct electron transfer of cytochrome c immobilized on a NaY zeolite matrix and its application in biosensing, Electrochim. Acta 49 (2004) 2139–2144.
[36] J.-H. Yu, H.-X. Ju, Preparation of porous titania sol-gel matrix for immobilization of horseradish peroxidase by a vapor deposition method, Anal. Chem. 74 (2002) 3579–3583.
[37] X. Qu, X. Dong, Z. Cheng, T. Lu, S. Dong, The direct electrochemistry of cytochrome c at the nanometer-sized rare earth element oxide particle-modified gold electrodes, J. Mol. Catal., A Chem. 106 (1996) 1–5.
[38] O. Ikeda, M. Ohtani, T. Yamaguchi, A. Komura, Direct electrochemistry of cytochrome c at a glassy carbon electrode covered with a microporous alumina membrane, Electrochim. Acta 43 (1998) 833–839.
[39] E. Topoglidis, T. Utz, R.L. Willis, C.J. Barnett, A.E.G. Gass, J.R. Durrant, Protein adsorption on nanoporous TiO_2 films: a novel approach to studying photoinduced protein/electrode transfer reactions, Faraday Discuss. 116 (2000) 35–46.
[40] Q. Li, G. Lou, J. Feng, Direct electron transfer for heme proteins assembled on nanocrystalline TiO_2 film, Electroanalysis 13 (2001) 359–363.
[41] H. Ju, S. Liu, B. Ge, F. Lisdat, F.W. Scheller, Electrochemistry of cytochrome c immobilized on colloidal gold modified carbon paste electrodes and its electrocatalytic activity, Electroanalysis 14 (2002) 141–147.
[42] G. Zhao, Z. Yin, L. Zhang, X. Wei, Direct electrochemistry of cytochrome c on a multi-walled carbon nanotubes modified electrode and its electrocatalytic activity for the reduction of H_2O_2, Electrochem. Commun. 7 (2005) 256–260.
[43] Q. Zhao, D. Zhan, H. Ma, M. Zhang, Y. Zhao, P. Jing, Z. Zhu, X. Wan, Y. Shao, Q. Zhuang, Direct proteins electrochemistry based on ionic liquid mediated carbon nanotube modified glassy carbon electrode, Front. Biosci. 10 (2005) 326–334.
[44] N. Sun, L. Guan, Z. Shi, N. Li, Z. Gu, Z. Zhu, M. Li, Y. Shao, Ferrocene Peapod Modified Electrodes: Preparation, Characterization, and Mediation of H_2O_2, Anal. Chem. 78 (2006) 6050–6057.
[45] B.R. Azamian, J.J. Davis, K.S. Coleman, C.B. Bagshaw, M.L.H. Green, Bioelectrochemical single-walled carbon nanotubes, J. Am. Chem. Soc. 124 (2002) 12664–12665.
[46] J.J. Davis, K.S. Coleman, B.R. Azamian, C.B. Bagshaw, M.L.H. Green, Chemical and biochemical sensing with modified single walled carbon nanotubes, Chem. Eur. J. 9 (2003) 3732–3739.
[47] N.W.S. Kam, H.J. Dai, Carbon nanotubes as intracellular protein transporters: generality and biological functionality, J. Am. Chem. Soc. 127 (2005) 6021–6026.
[48] H.A. Heering, K.A. Williams, S. de Vries, C. Dekker, Specific vectorial immobilization of oligonucleotide-modified yeast cytochrome c on carbon nanotubes, ChemPhysChem 7 (2006) 1705–1709.
[49] P.L. Edmiston, J.E. Lee, S.-S. Cheng, S.S. Saavedra, Molecular orientation distributions in protein films. 1. Cytochrome c adsorbed to substrates of variable surface chemistry, J. Am. Chem. Soc. 119 (1997) 560–570.
[50] P. Hildebrandt, D.H. Murgida, Electron transfer dynamics of cytochrome c bound to self-assembled monolayers on silver electrodes, Bioelectrochem. 55 (2002) 139–143.
[51] K. Niki, W.R. Hardy, M.G. Hill, H. Li, J.R. Sprinkle, E. Margoliash, K. Fujita, R. Tanimura, N. Nakamura, H. Ohno, J.H. Richards, H.B. Gray, Coupling to lysine-13 promotes electron tunneling through carboxylate-terminated alkanethiol self-assembled monolayers to cytochrome c, J. Phys. Chem., B 107 (2003) 9947–9949.
[52] J. Zhou, J. Zheng, S. Jiang, Molecular simulation studies of the orientation and conformation of cytochrome c adsorbed on self-assembled monolayers, J. Phys. Chem., B 108 (2004) 17418–17424.
[53] J. Liu, M.J. Casavant, M. Cox, D.A. Walters, P. Boul, W. Lu, A.J. Rimberg, K.A. Smith, D.T. Colbert, R.E. Smalley, Controlled deposition of individual single-walled carbon nanotubes on chemically functionalized templates, Chem. Phys. Lett. 303 (1999) 125–129.
[54] J. Kong, H.J. Dai, Full and modulated chemical gating of individual carbon nanotubes by organic amine compounds, J. Phys. Chem., B 105 (2001) 2890–2893.
[55] E. Valentin, S. Auvray, J. Goethals, J. Lewenstein, L. Capes, A. Filoramo, A. Ribayrol, R. Tsui, J.-P. Bourgoin, J.-N. Patillon, high-density selective placement methods for carbon nanotubes, Microelectron. Eng. 61 (2002) 491–496.
[56] H. Pilletier, J. Kraut, Crystal structure of a complex between electron transfer partners, cytochrome c peroxidase and cytochrome c, Science 258 (1992) 1748–1755.
[57] J.A.R. Worrall, U. Kolczak, G.W. Canters, M. Ubbink, Interaction of Yeast Iso-1-cytochrome c with cytochrome c peroxidase investigated by [^{15}N, ^{1}H] heteronuclear NMR spectroscopy, Biochemistry 40 (2001) 7069–7076.
[58] C. Hunte, S. Solmaz, C. Lange, Electron transfer between yeast cytochrome bc1 complex and cytochrome c: a structural analysis, Biochim. Biophys. Acta 1555 (2002) 21–28.
[59] S. Dopner, P. Hildebrandt, F.I. Rosell, A.G. Mauk, M. von Walter, G. Buse, T. Soulimane, The structural and functional role of lysine residues in the binding domain of cytochrome c in the electron transfer to cytochrome c oxidase, Eur. J. Biochem. 261 (1999) 379–391.
[60] V.A. Roberts, M.E. Pique, Definition of the interaction domain for cytochrome c on cytochrome c oxidase. III. prediction of the docked complex by a complete, systematic search, J. Biol. Chem. 274 (1999) 38051–38060.
[61] D. Flock, V. Helms, Protein-protein docking of electron transfer complexes-cytochrome c oxidase and cytochrome c, Proteins 47 (2002) 75–85.
[62] B.E. Conway, M.A. Sattar, D. Gilroy, Electrochemistry of the nickel-oxide electrode—V. Self-passivation effects in oxygen-evolution kinetics, Electrochim. Acta 14 (1969) 677–694.
[63] M.A. Sattar, B.E. Conway, Electrochemistry of the nickel-oxide electrode—VI. Surface oxidation of nickel anodes in alkaline solution, Electrochim. Acta 14 (1969) 695–710.
[64] B.E. Conway, M.A. Sattar, D. Gilroy, Electrochemistry of the nickel-oxide electrode—VII. Potentiostatic step method for study of adsorbed intermediates, Electrochim. Acta 14 (1969) 711–724.
[65] B.E. Conway, M.A. Sattar, Electrochemistry of the nickel oxide electrode : Part VIII. Stoichiometry of thin film oxide layers, J. Electroanal. Chem. 19 (1968) 351–364.
[66] M. Fleischmann, K. Korinek, D. Pletcher, The oxidation of organic compounds at a nickel anode in alkaline solution, J. Electroanal. Chem. 31 (1971) 39–49.
[67] J.V. Dobson, B.R. Chapman, The electrode kinetic behaviour of nickel in aqueous stearic acid salt media up to 210 °C, Electrochim. Acta 32 (1987) 415–418.
[68] G. Cordeiro, O.R. Matos, O.E. Barcia, L. Beaunier, C. Deslouis, B. Tribollet, Anodic dissolution of nickel in concentrated sulfuric acidic solutions, J. Appl. Electrochem. 26 (1996) 1083–1092.
[69] I. Epelboin, M. Keddam, Kinetics of formation of primary and secondary passivity in sulphuric aqueous media, Electrochim. Acta 17 (1972) 177–186.
[70] A. Jouanneau, M. Keddam, M.C. Petit, A general model of the anodic behaviour of nickel in acidic media, Electrochim. Acta 21 (1976) 287–292.
[71] J.R. Vilche, A.J. Arvia, Kinetics and mechanism of the nickel electrode—II. Acid solutions containing a high concentration of sulphate and nickel ions, Corros. Sci. 18 (1978) 441–463.

[72] S.G. Real, J.R. Vilche, A.J. Arvia, The characteristics of the potentiodynamic potential/current profiles obtained with the Ni/0.5N H_2SO_4 interface. A contribution to the mechanism of the electrode process, Corros. Sci. 20 (1980) 563–586.
[73] M.R. Barbosa, S.G. Real, J.R. Vilche, A.J. Arvia, Comparative potentiodynamic study of nickel in still and stirred sulfuric acid-potassium sulfate solutions in the 0.4–5.7 pH range, J. Electrochem. Soc. 135 (1988) 1077–1084.
[74] S.G. Real, M.R. Barbosa, J.R. Vilche, A.J. Arvia, Influence of chloride concentration on the active dissolution and passivation of nickel electrodes in acid sulfate-solutions, J. Electrochem. Soc. 137 (1990) 1696–1702.
[75] M.R. Barbosa, J.A. Bastos, J.J. Gracia-Jareno, F. Vicente, Chloride role in the surface of nickel electrode, Electrochim. Acta 44 (1998) 957–965.
[76] R.S. Schrebler Guzman, J.R. Vilche, A.J. Arvia, The potentiodynamic behaviour of nickel in potassium hydroxide solutions, J. Appl. Electrochem. 8 (1978) 67–70.
[77] R.S. Schrebler Guzman, J.R. Vilche, A.J. Arvia, Rate processes related to the hydrated nickel hydroxide electrode in alkaline solutions, J. Electrochem. Soc. 125 (1978) 1578–1583.
[78] R.S. Schrebler Guzman, J.R. Vilche, A.J. Arvia, Electrochemical and chemical reactions involving non-equilibrium species at the nickel hydroxide electrode, J. Appl. Electrochem. 9 (1979) 321–327.
[79] B. MacDougall, M. Cohen, Anodic oxide films on nickel in acid solutions, J. Electrochem. Soc. 123 (1976) 191–197.
[80] M.A. Hopper, J.L. Ord, An optical study of the growth and oxidation of nickel hydroxide films, J. Electrochem. Soc. 120 (1973) 183–187.
[81] J.F. Wolf, L.-S.R. Yeh, A. Damanjanovic, Anodic oxide films at nickel electrodes in alkaline solutions—I. Kinetics of growth of the β-$Ni(OH)_2$ phase, Electrochim. Acta 26 (1981) 409–416.
[82] J.F. Wolf, L.-S.R. Yeh, A. Damanjanovic, Anodic oxide films at nickel electrodes in alkaline solutions—II. pH dependence and rate determining step, Electrochim. Acta 26 (1981) 811–817.
[83] J.L. Weininger, M.W. Breiter, Effect of crystal structure on the anodic oxidation of nickel, J. Electrochem. Soc. 110 (1963) 484–490.
[84] D. Giovanelli, N.S. Lawrence, L. Jiang, T.G.J. Jones, R.G. Compton, Electrochemical determination of sulphide at nickel electrodes in alkaline media: a new electrochemical sensor, Sens. Actuators, B, Chem. 88 (2003) 320–328.
[85] D. Giovanelli, N.S. Lawrence, L. Jiang, T.G.J. Jones, R.G. Compton, Amperometric determination of sulfide at a pre-oxidised nickel electrode in acidic media, Analyst 128 (2003) 173–177.
[86] R.D. Tilley, D.A. Jefferson, The synthesis of nickel sulfide nanoparticles on graphitized carbon supports, J. Phys. Chem., B 106 (2002) 10895–10901.
[87] J.L. Wong, M. Tian, W.R. Jin, Y.N. He, Speciation of sulfidic nickel by carbon paste electrode voltammetry. Determination of Ni_3S_2 in solid mixtures, Electroanalysis 12 (2001) 1355–1359.
[88] D. Giovanelli, N.S. Lawrence, S.J. Wilkins, L. Jiang, T.G.J. Jones, R.G. Compton, Anodic stripping voltammetry of sulphide at a nickel film: towards the development of a reagentless sensor, Talanta 61 (2003) 211–220.
[89] A. Salimi, E. Sharifi, A. Noorbakhsh, S. Soltanian, Direct voltammetry and electrocatalytic properties of hemoglobin immobilized on a glassy carbon electrode modified with nickel oxide nanoparticles, Electrochem. Commun. 8 (2006) 1499–1508.
[90] A. Salimi, E. Sharifi, A. Noorbakhsh, S. Soltanian, Direct electrochemistry and electrocatalytic activity of catalase immobilized onto electrodeposited nano-scale islands of nickel oxide, Biophys. Chem. 125 (2007) 540–548.
[91] A. Salimi, E. Sharifi, A. Noorbakhsh, S. Soltanian, Immobilization of glucose oxidase on electrodeposited nickel oxide nanoparticles: Direct electron transfer and electrocatalytic activity, Biosens. Bioelectron. 22 (2007) 3146–3153.
[92] C. Mu, Q. Zhao, D. Xu, Q. Zhuang, Y. Shao, Silicon nanotube array/gold electrode for direct electrochemistry of cytochrome c, J. Phys. Chem., B 111 (2007) 1491–1495.
[93] S. Suzen, B.T. Dermircigil, S.A. Ozkan, S. Suzen, B.T. Dermircigil, S.A. Ozkan, Electroanalytical evaluation and determination of 5-(3-indolyl)-2-thiohydantoin derivatives by voltammetric studies: possible relevance to in vitro metabolism, New J. Chem. 6 (2003) 1007–1011.
[94] R.M. Ottenbrite, E. Chiellini (Eds.), Polymers in Medicine: Biomedical and Pharmaceutical Applications, Technomic Publishing, Lancaster, PA, 1992.
[95] A.E. Kasmi, M.C. Leopold, R. Galligan, R.T. Robertson, S.S. Saavedra, K.E. Kacemi, E.F. Bowden, Adsorptive immobilization of cytochrome *c* on indium/tin oxide (ITO): electrochemical evidence for electron transfer-induced conformational changes, Electrochem. Commun. 4 (2002) 177–181.
[96] C. Xiang, Y. Zou, L.-X. Sun, F. Xu, Direct electrochemistry and electrocatalysis of cytochrome c immobilized on gold nanoparticles-chitosan-carbon nanotubes modified electrode, Talanta (2007), doi:10.1016/j.talanta.2007.05.050.
[97] E. Laviron, General expression of the linear potential sweep voltammograms in the case of diffusion less electrochemical systems, J. Electroanal. Chem. 101 (1979) 19–28.
[98] E. Laviron, The use of linear potential sweep voltammetry and of AC voltammetry for the study of the surface electrochemical reaction of strongly adsorbed systems and of redox modified electrodes, J. Electroanal. Chem. 100 (1979) 263–270.